How strong are H-bonds at the fully hydroxylated silica surfaces? Insights from the B3LYP electron density topological analysis

How Strong are H-bonds at the Fully Hydroxylated Silica Surfaces? Insights from the B3LYP Electron Density Topological Analysis

Federico Musso[1)], Silvia Casassa[2)], Marta Corno[2)] and Piero Ugliengo*[2)]

[1)]Intelligent Pharma, Parc Científic de Barcelona, Carrer Baldiri Reixac 4, 08028 Barcelona, Spain. [2)]University of Torino, Dipartimento di Chimica and NIS, Nanostructured Interfaces and Surface, Centre, Via P. Giuria 7 – I-10125 Torino, Italy. *Corresponding author: piero.ugliengo@unito.it

Abstract

The calculation through the supermolecular approach of the hydrogen bond strength E_{HB} between silanol groups at the surface of an ample class of silica-based materials is hindered by the intrinsic difficulty to define the "H-bond free" reference system. We propose, for the first time, to evaluate E_{HB} by adopting the literature empirical correlation relating the Bader local electronic kinetic energy density G_b computed at the H···O bond critical point with E_{HB}. Remarkably, E_{HB} for the hydroxylated surfaces of quartz polymorphs correlates with surface formation energy, showing the that surface E_{HB} is responsible of the surface stability. A number of correlations between hydrogen bond features are established, with that between E_{HB} and the enhanced infrared intensity associated to surface hydrogen bond formation, obeying the literature formula semi-quantitatively. The present results are quite general and can be extended to other inorganic surfaces where hydrogen bonds between surface sites are the dominant features.

Keywords: crystalline silica surfaces; B3LYP-D*; hydrogen bond strength; Bader topological analysis; surface silanols.

Introduction

Hydrogen bond (H-bond) is one of the most important and studied interactions.[1] Its existence imparts peculiar properties to liquid and solid water, allows the correct DNA base pairing, drives the conformation of the tertiary structure of proteins, is a key structural motif in many molecular crystals and plays a fundamental role in thin-layer chromatography based on silica supports. One of the most important features of H-bonded systems is its energy strength. It is the energy gained by a system when passing from a state without H-bonds (free constituents) to a molecular aggregate held by H-bond interactions. Examples of these situations are the water dimer, a larger aggregate of water molecules (a cluster) up to liquid and crystalline water. The huge number of possible molecular situations occurring, for instance, in molecular crystals is well described in Reference[1]. The H-bond strength can be computed by a large variety of computational approaches, from molecular mechanics up to high level of theory, like the golden standard CCSD(T) method.[2] Within the supermolecular approach, the interaction energy E_{HB} of an hydrogen bonded AH···B system 1) is given by equation 2):

$$AH + B \rightarrow AH\cdots B \qquad 1)$$

$$E_{HB} = E(AH\cdots B) - E(AH) - E(B) \qquad 2)$$

E(AH···B), E(AH) and E(B) are the total energies of the H-bonded system and the spatially infinite separated AH and B constituents. For a bound system, E_{HB} is a negative quantity and includes all the intermolecular components of the interaction between AH and B moieties. The supermolecular approach assumes the separability of the constituents of the H-bonded aggregate. For molecular clusters, liquids or molecular crystals the free constituent are straightforwardly identifiable. For instance, the cohesive energy of water ice is the total energy of the ice unit cell content minus the energy of a corresponding number of free water molecules. A completely different situation occurs when H-bond interactions develop at the surface of hydroxylated inorganic materials: here, no free reference state is definable. A specific example

are the fully hydroxylated silica surfaces derived from the crystalline quartz polymorphs or amorphous silica. In both cases, the abundant Si-OH groups engage in a complex web of H-bond interactions made of dimers, rings or infinite extended H-bonded 2D patterns. We have recently characterized the structural and vibrational features of these systems, which are also the targets of the present work.[3,4] In that work, we estimated the H-bond strength using a rather rough approach in which arbitrary cluster models where cut out from the surfaces.

Scheme 1 highlights the difficulty in defining a non-interacting reference system for surfaces in which H-bonding takes place. As shown, it is almost impossible to break surface H-bonds without introducing an artificial energy penalty due to the extra repulsion between the non-interacting pairs (see blue arrows in Scheme 1) biasing, in an unpredictable way, the final E_{HB} value. Other arrangements will bring to one of the many H-bonding patterns at the silica surfaces (vide infra and Fig. 2).

Methods

In this work, we provide a possible way out of the problem described in the introduction by relying on Bader analysis of the H-bond features, which allows to evaluate the E_{HB} term by avoiding the supermolecular approach. We rely on literature empirical correlations between the local electronic kinetic energy density G_b computed at the critical point *b* inside the region of the H···B bond, within the context of Bader topological analysis.[5-7] Vener and co-workers[5] have recently tested the validity of this method on a set of H-bonded molecular crystals, by comparing the DFT value of E_{HB} (computed with the supermolecule approach) with the local kinetic energy G_b computed by periodic DFT calculations or estimated from precise X-ray diffraction experiments.

The relationship introduced by Mata et al.[6] and adopted by Vener et al.[5] which is relevant for the present work is:

$$E_{HB} = 1126.3\ G_b \qquad (\text{kJ mol}^{-1}) \qquad 3)$$

For H-bond occurring at the silica surfaces, as in the present work, we can rigorously compute the G_b value, which is an intrinsic property of each H-bond and then directly arrive to E_{HB} through formula 3). A second interesting and general correlation has been proposed in the literature between the $\Delta\omega$ frequency shift suffered by a H-bond donor compared to the free vibrating AH group and the E_{HB} values:[8]

$$E_{HB} = 1.3\ \Delta\omega(OH)^{1/2} \quad (kJ\ mol^{-1}) \qquad 4)$$

This relationship has been tested for a relatively wide frequency shift interval ($\Delta\omega$(OH) from 20 to 2500 cm^{-1}) on a number of molecular crystals and simple dimers.[9] The existence of rather strong H-bond between silanol groups at the crystalline silica surfaces, as testified by large bathochromic shift of the silanol OH vibrational frequency, has been reported since long ago by Bolis *et al* for α-quartz and different amorphous silica samples.[10]

In the following, we will show how to use relations 3) and 4) to characterize the hydroxylated silica surfaces derived from the quartz polymorphs.

Models

The studied surfaces derive from the corresponding silica bulks (α-quartz (Q), β-cristobalite (C) and tridymite (T)), by cutting slab models of variable thickness, cell parameters and number of atoms inside the unit cell. The unsatisfied Si or SiO valences of the derived surface are saturated with OH groups or H atoms, respectively, using the molecular graphic program MOLDRAW,[11] also used for the visualization and the geometrical manipulation of all the structures. As the model slab features two equivalent faces, we limited the analysis of structural and vibrational frequencies (*vide infra*) to one face only. The set of resulting surfaces have already been studied in the past by some of us,[3] but for the addition of the tridymite T(010) and the removal of the quartz Q(101) slab structures (the latter due to convergence problems).

Computational details

We used the *ab initio* CRYSTAL14 code[12,13] for all calculations. This code implements the Hartree-Fock and Kohn-Sham self-consistent field methods for the study of periodic systems[14] in a basis set of Gaussian type orbitals (GTO) and allows full geometry optimization (both internal coordinates and cell size[15]) of molecules and crystals.

The GTO basis set, used for the geometry optimization of all the structures, consists of the triple-ζ quality basis set developed by Ahlrichs and co-workers[16] supplemented by a set of polarization functions on all atoms. In agreement with previous works,[3,17] the B3LYP-D* hybrid exchange-correlation functional[18,19] has been adopted for all calculations, in which the D* is the Grimme's correction for dispersive interactions as modified for molecular crystals.[17] We tighten the convergence criteria to accurate locate the potential energy minima needed for the subsequent Bader analysis. The Hamiltonian matrix has been diagonalized[20] in 10 reciprocal lattice points (*k*-points), corresponding to a shrinking factor of 4,[21] while for bulk tridymite, the shrink factor was set to 6 (52 reciprocal *k*-points).

Following previous experience,[22] the complete phonon frequencies calculation of the hydroxylated surfaces is restricted to the Hessian matrix of the Si-OH fragments only. For all considered cases, we checked that the computed harmonic frequencies were all positive ensuring that the slab models are all minima on the B3LYP potential energy surface, at least within the considered ensemble of Si-OH fragments. Infrared intensity for each normal mode was obtained by computing the dipole moment variation along the normal mode, adopting the Berry phase method.[23]

We adopted an updated version of the program TOPOND13,[24,25] as encoded into the last release of the CRYSTAL14 code, to perform the charge density topological analysis according to the Quantum Theory of Atoms in Molecules, developed by Richard Bader[26] and extended to crystals by co-workers.[27] The search of the electron density critical points has been pursued

using a sophisticate eigenvector following approach[28,29] in a finite region of space, which encloses a molecular cluster built up around each non-equivalent atom inside the cell.

Results and discussion

Fig. 1 shows the treated systems and highlights a number of possible H-bond patterns: infinite chains of H-bonds (C-inf) as in Q(001), Q(100), C(101) and T(110); H-bonded dimers (D) as in Q(010), Q(011), C(001), T(010) and T(100); H-bonded rings (R) as in C(110) and isolated silanol (I) as in C(100) and T(001). It is apparent that H-bond length depends on this kind of organization. For each structure, the Bader analysis locates the *b* electron density bond critical point for each OH···O interaction, by the automatic search implemented in TOPOND13 described in the Computational Details section. At the bond critical points, we computed the local electronic kinetic energy G_b and by equation 3) we computed the E_{HB} values. Relevant data are reported in Tab. 1.

E_{HB} *versus* H-bond geometrical features

Following Mata et al suggestions,[6] we correlate the H···O bond distance with the E_{HB} values (see Tab. 1), as shown in Fig. 2. Data for all considered cases nicely fit to:

$$E_{HB} = 994.3\ (H\cdots O)^{-5.69} \qquad 4)$$

curve. Data are all distributed almost uniformly regardless the considered silica polymorph, showing the universal nature of H-bond features. The dashed curve of Fig. 2 refers to the Vener empirical equation derived from molecular crystals:

$$E_{HB} = 150.4\ (H\cdots O)^{-3.05} \qquad 5)$$

The discrepancy between the two curves may be due to the special H-bond structural features for the present case, which is rather different from the dataset developed for regular H-bonded systems like simple dimers and molecular crystals, in which the surface constraints imposed by the underlying bulk are absent. Indeed, following Vener's indication, its formula is bound to underestimate by 15% the E_{HB}, in agreement with the trend of our data. Nevertheless, the E_{HB}

values are in the range of the expected H-bond strength. Very recently, a similar approach has been used by Tsendra *et al* [30] to estimate the H-bond strength between silanol groups at the (100) α-quartz surface, to be contrasted with the competing H-bond interaction with nitrogen-containing adsorbed molecules.

E_{HB} *versus* H-bond vibrational features

A further correlation, shown in Fig. 3, is performed between $\Delta\omega(OH)$ and E_{HB}, following the Iogansen's proposal[8] and Rozenberg's work.[9] Data are averaged over close enough structures to smear out small fluctuations and have been aggregated by the kind of motif to which the H-bonds belong. The solid curve is the best fit of our data with the $E_{HB} = 0.55\ \Delta\omega(OH)^{0.65}$ curve, whereas the one from literature[8] $E_{HB} = 1.3\ \Delta\omega(OH)^{½}$ is shown as dashed line. As for the previous correlation, the two curves are different, reflecting different behavior for H-bond in molecular systems compared to surface H-bonds. Remarkably, the region of higher vibrational shifts is the one deviating more from the two curves, irrespective on a given H-bond pattern. We believe this is partially due to the missing anharmonic effect in the computed OH stretching, which is important for OH groups in H-bond interactions as shown in previous work.[31,32] Correcting the frequencies by scaling the harmonic frequencies is not straightforward, as the OH anharmonicity is a subtle function of H-bond strength.

Fig. 4 shows the correlation between the $<E_{HB}>$ and $<A(OH)^{½}\text{-}A_0(OH)^{½}>$, in which A(OH) and $A_0(OH)$ are, respectively, the infrared intensity of a specific surface OH bond and that for the free silanol molecule, chosen as the H-bond free state. The correlation is rather robust (r^2=0.87) resulting in $<E_{HB}> = 10.7\ <A(OH)^{½}\text{-}A_0(OH)^{½}>$ to be compared with the literature empirical relationship derived by Iogansen[8] on a large set of experimental data which reads $<E_{HB}> = 12.2\ <A(OH)^{½}\text{-}A_0(OH)^{½}>$.

All correlations previously discussed deviate to some extent from that derived from molecular aggregates or molecular crystals. We suspect this is due to the geometrical constraints imposed on the Si-OH surface groups by the underlying oxide bulk which does not allow the surface hydrogen bond features to be fully exploited.

E_{HB} *versus* surface energy

An interesting question is whether the E_{HB} values can be related to the formation energy EF_{SURF} of each surface from the corresponding bulk. This quantity has been computed for the considered surfaces by some of us in the past.[3] The process to arrive at the EF_{SURF} is the following:

$$a\ \text{Bulk}(SiO_2) + b\ H_2O \rightarrow c\ \text{Slab}(SiOH) \qquad 5)$$

$$EF_{SURF} = c\ E(\text{Slab}) - [a\ E(\text{Bulk}) + b\ E(H_2O)] \qquad 6)$$

in which E(Slab) and E(Bulk) are the electronic energies *per* unit cell of the considered slab and its corresponding bulk phase, while $E(H_2O)$ is the energy of a free optimized water molecule. Now, for a specific surface, a number of H-bonds are present at the upper/lower face of the slab. Therefore, the total H-bond energy for a given surface is the sum of the average of all distinct H-bond energy E_{HB} contributions, $\sum\langle E_{HB}\rangle$. Fig. 5 correlates the average EF_{SURF} with the $\sum\langle E_{HB}\rangle$ values. Remarkably, the correlation is rather good (r^2=0.90) and the best fit gives $\sum\langle E_{HB}\rangle$ =1.1 EF_{SURF}, *i.e.* an almost direct relationship between the strength of the surface H-bonds and the surface formation energy. This means that the surface formation energy is, largely, independent from the internal slab relaxation with respect to the bulk. Therefore, it is the strength of the surface H-bond bond pattern that drives the surface formation.

Conclusions

In this work, we propose a new method to estimate the strength of the hydrogen bond (E_{HB}) between silanol Si-OH groups at the surfaces of crystalline silica polymorphs. The classical recipe to compute E_{HB} for molecular aggregates based on the supermolecular approach assumes to define the "free state" for the interacting constituents. For hydrogen bonds occurring at the silica surface the "free state" is hill or not definable at all, so that the supermolecular approach does not apply. Therefore, we resorted to an empirical relationship, rigorously based on Bader topological analysis and suggested by Mata et al,[6] which establish the relationship between E_{HB} and the local electronic kinetic energy G_b at the H···O bond critical point, i.e. $E_{HB} = 1126.3\ G_b$. We showed that all the important empirical relationships proposed in the literature for molecular aggregates and relating E_{HB} with the H···O bond distance, the OH frequency shift and the OH infrared intensity are obeyed also for H-bonds at silica surfaces. We revealed some deviations from the proposed behaviour derived for the molecular cases due to the geometrical constraints imposed by the underlying bulk silica on the surface SiOH sites. We also proved that the total strength of the H-bond energy computed as the sum of all E_{HB} contributions of each surface H···O bond, is almost proportional to the surface formation energy. This is particularly relevant, as it means that the network of H-bonds at silica surfaces drives the energetic of its surface formation. We suspect that the latter result is more general than the context of silica surfaces and may hold for the hydroxylated surfaces of other important oxides.

Acknowledgements

Authors are very grateful to Prof. Carlo Gatti (CNR, Milano) for useful discussion and assistance. Compagnia di San Paolo and University of Turin are gratefully acknowledged for funding Project ORTO114XNH through ''Bando per il finanziamento di progetti di ricerca di Ateneo – anno 2011''.

Table 1. For each considered surface the reported quantities are: <(H···O)> the average H-bonding distance, <G_b> the average local electronic kinetic energy density computed at the *b* H···O critical point, <E_{HB}> the average hydrogen bond interaction energy, <ω(OH)> the average OH harmonic frequency and <Δω(OH)> the average OH frequency shift with respect to free silanol. For all cases, the average refers to the specific property of almost equivalent H···O bonds occurring on the two faces of the modelled slab surface. See Fig. 1 for surface details.

Surface	<(H···O)> Å	<G_b> au	<E_{HB}> kJ mol^{-1}	<ω(OH)> cm^{-1}	<Δω(OH)> cm^{-1}
Q(001)	1.866	0.024959	28.1[b)]	3522	365[a)]
	2.078	0.014045	15.8	3620	266
	1.998	0.017422	19.6	3612	274
Q(010)	2.175	0.011233	12.7	3718	168
Q(100)	1.779	0.031887	35.9	3476	410
	2.218	0.010700	12.1	3688	198
Q(011)	2.028	0.016661	18.8	3735	152
C(001)	1.704	0.038271	43.1	3455	431
C(100)	3.458	0.000688	0.8	3853	33
C(101)	2.138	0.012749	14.4	3668	218
	2.179	0.010738	12.1	3711	176
C(110)	2.105	0.013061	14.7	3636	250
	1.801	0.029904	33.7	3517	369
T(010)	2.059	0.014707	16.6	3692	194
T(110)	1.935	0.020473	23.1	3549	338
	1.995	0.017228	19.4	3564	322
	1.941	0.020088	22.6	3556	330
	1.951	0.019457	21.9	3551	335
T(100)	1.894	0.023115	26.0	3638	248

a) Frequency shift computed with respect to the harmonic frequency value of 3886 cm^{-1} obtained for the free silanol molecule (H_3SiOH).

b) Computed with the empirical formula E_{HB}=1125.3 G_b (kJ mol^{-1}).

Figures Captions

Scheme 1. Different H-bonded situations. Top: the classical H-bond for the water dimer. Bottom: the H-bond between surface silanols at the (101) fully hydroxylated cristobalite surface and one possible configuration with broken H-bonds.

Fig. 1. Top view of the unit cell of the studied hydroxylated silica surfaces. Q, C and T refer to α-quartz, β-cristobalite and tridymite silica polymorphs, respectively. OH groups shown as red/grey balls. Hydrogen bond depicted as dashed lines in units of Å.

Fig. 2. Average H···O distances <H···O> *vs* average hydrogen bond energy $<E_{HB}>$ grouped by polymorph (Q, C and T) surfaces. Best fit continuous curve $E_{HB} = 994.3\ (H\cdots O)^{-5.69}$. Dashed curve $E_{HB} = 150.4\ (H\cdots O)^{-3.05}$ after Vener et al (Ref. [5]). See Tab. 1 caption for the definition of average values.

Fig. 3. Average $<\Delta\omega(OH)>$ frequency shift *vs* average hydrogen bond energy $<E_{HB}>$ for all polymorph surfaces grouped for isolated silanols (I), rings (R), dimers (D) and infinite chains (C-inf). Best fit continuous curve $E_{HB} = 0.55\ \Delta\omega(OH)^{0.65}$. Dashed curve $E_{HB} = 1.3\ \Delta\omega(OH)^{0.50}$ after Iogansen (Ref.[8]). See Tab. 1 caption for the definition of average values.

Fig. 4. Average $<E_{HB}>$ H-bond energies for equivalent H-bonds *vs* the average in the difference $A(OH)^{½}$-$A_0(OH)^{½}$ in which A(OH) and $A_0(OH)$ are, respectively, the infrared intensity of the OH bond involved in the H-bond interaction and that of the free silanol molecule. Best fit continuous line $<E_{HB}> = 10.7\ <A(OH)^{½}-A_0(OH)^{½}>$, $r^2=0.86$. See Tab. 1 caption for the definition of average values.

Fig. 5. Sum of average $\sum<E_{HB}>$ H-bond energies for all surface H-bonds of each silica surface *vs* the formation energy $-EF_{SURF}$ of each surface from the silica bulk and water. Best fit continuous line $\sum<E_{HB}> = -1.10\ EF_{SURF}$, $r^2=0.90$. See Tab. 1 caption for the definition of average values.

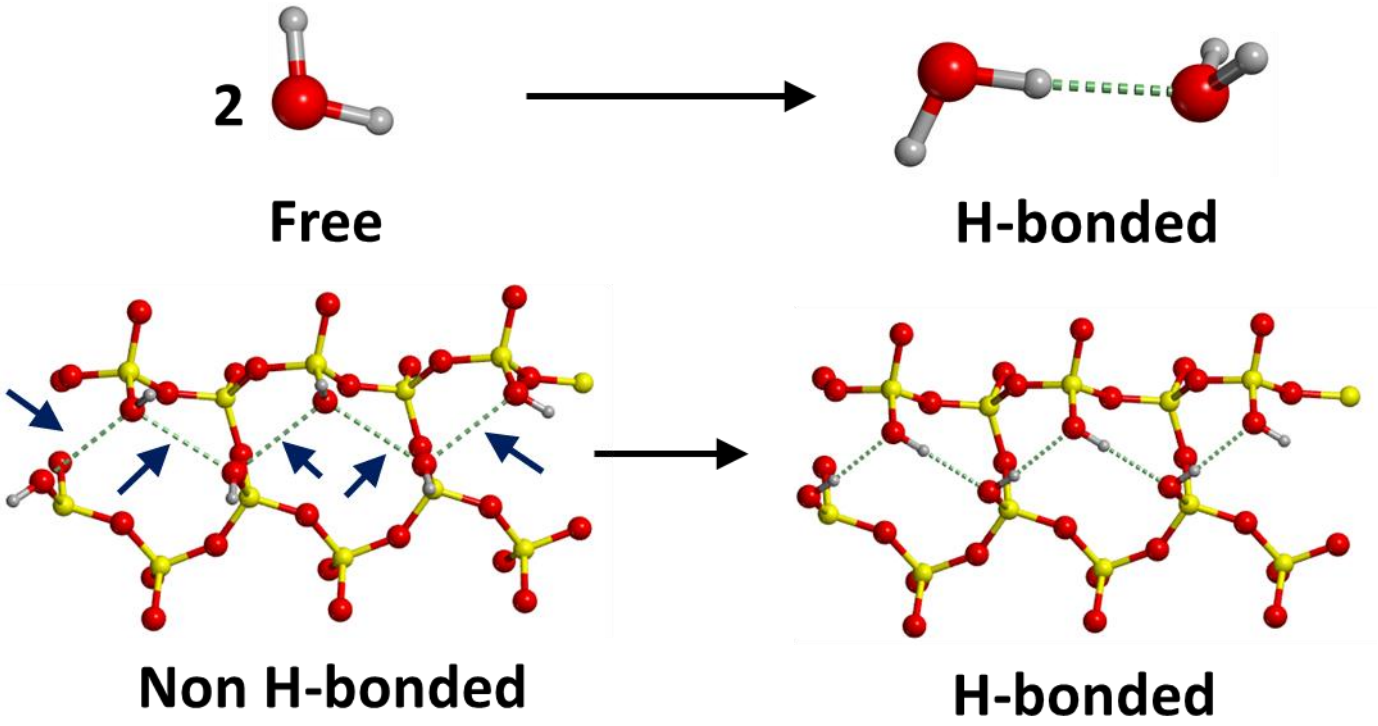

Scheme 1

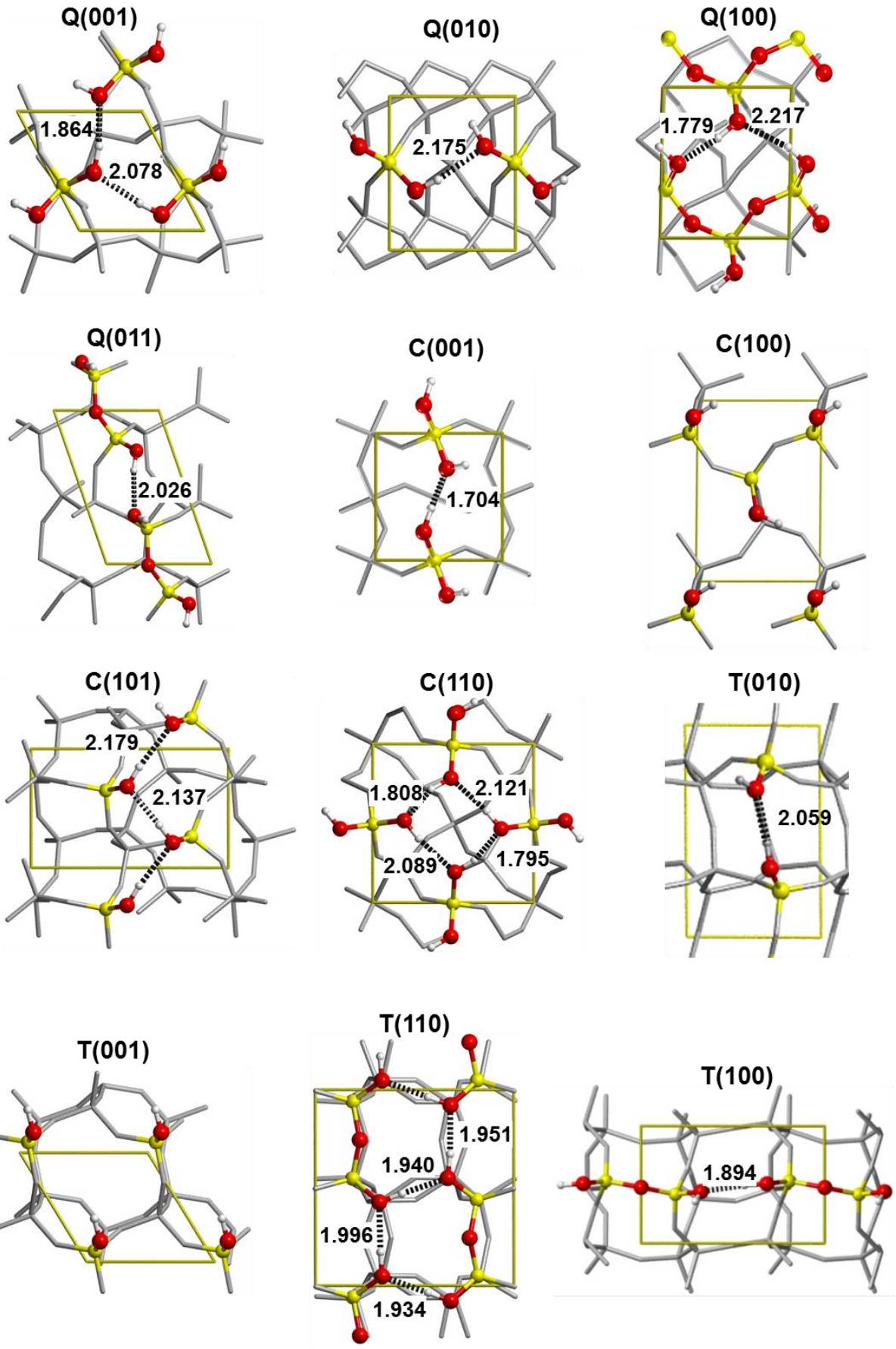
Q(001)
1.864
2.078
Q(010)
2.175
Q(100)
1.779
2.217
Q(011)
2.026
C(001)
1.704
C(100)
C(101)
2.179
2.137
C(110)
1.808
2.121
2.089
1.795
T(010)
2.059
T(001)
T(110)
1.951
1.940
1.996
1.934
T(100)
1.894

Figure 1

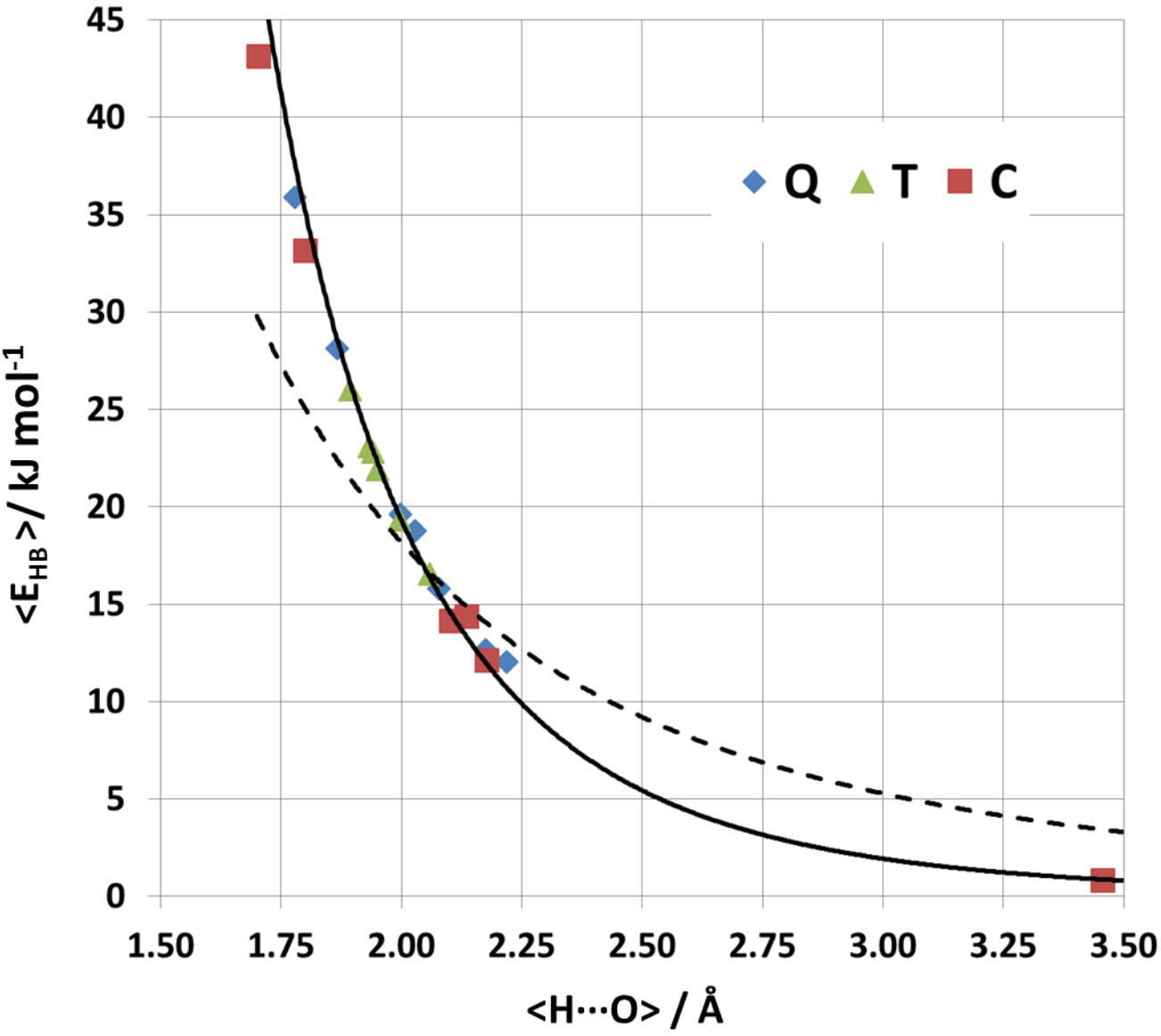
45
40
35
30
25
20
15
10
5
0
1.50
1.75
2.00
2.25
2.50
2.75
3.00
3.25
3.50
Q
T
C
<E_HB> / kJ mol-1
<H···O> / Å

Figure 2

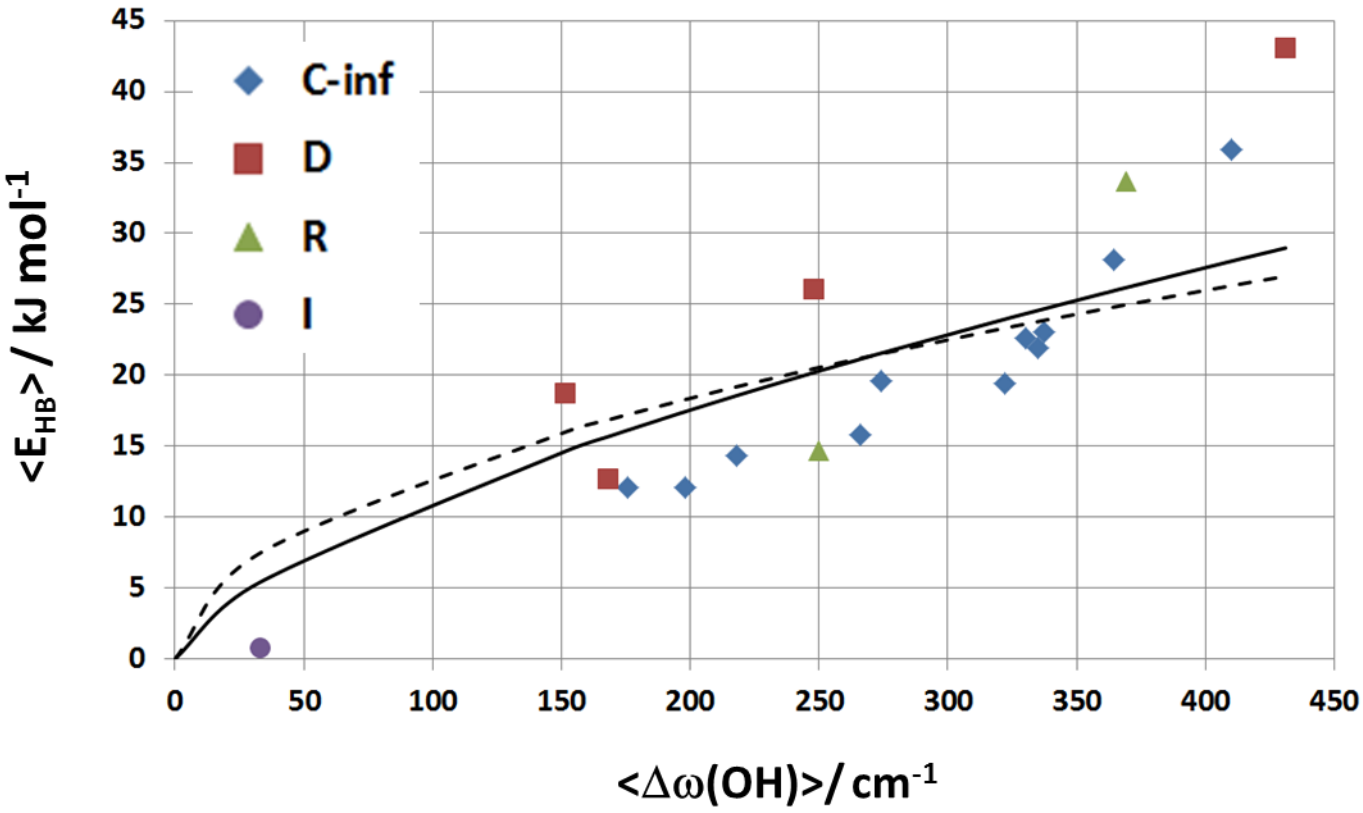
C-inf
D
R
I
45
40
35
30
25
20
15
10
5
0
0
50
100
150
200
250
300
350
400
450
<E_HB> / kJ mol-1
<Δω(OH)> / cm-1

Figure 3

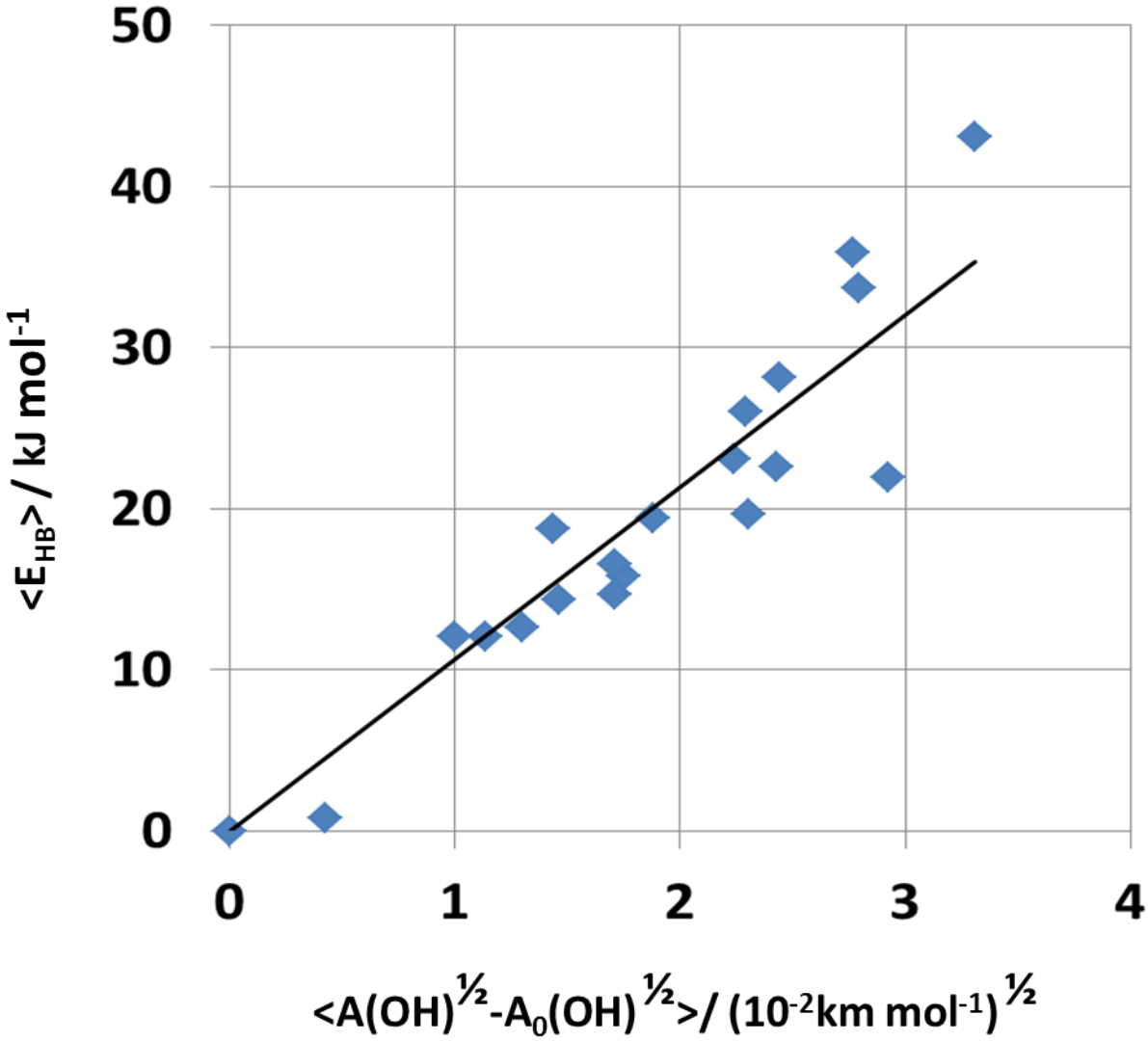

Figure 4

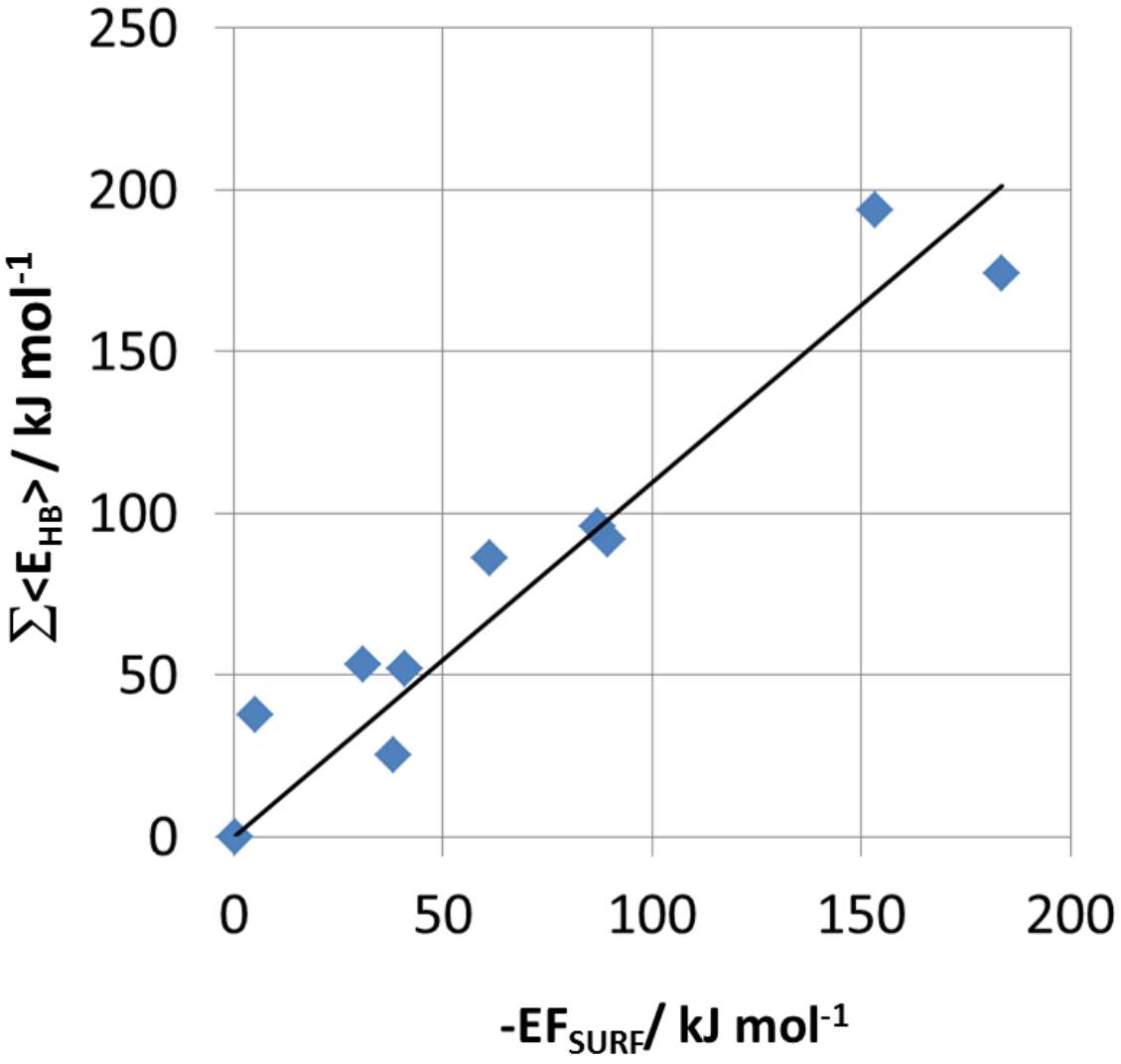

Figure 5

References

1. Gilli G, Gilli P (2009) The Nature of the Hydrogen Bond: Outline of a Comprehensive Hydrogen Bond Theory 1st edn. Oxford University Press, Oxford

2. Jensen F (1999) Introduction to computational chemistry. John Wiley & Sons Ltd, Chichester

3. Musso F, Sodupe M, Corno M, Ugliengo P (2009) H-Bond Features of Fully Hydroxylated Surfaces of Crystalline Silica Polymorphs: A Periodic B3LYP Study. J Phys Chem C 113 (41):17876-17884

4. Musso F, Ugliengo P, Sodupe M (2011) Do H-Bond Features of Silica Surfaces Affect the H_2O and NH_3 Adsorption? Insights from Periodic B3LYP Calculations. J Phys Chem A 115 (41):11221-11228. doi:Doi 10.1021/Jp203988j

5. Vener MV, Egorova AN, Churakov AV, Tsirelson VG (2012) Intermolecular hydrogen bond energies in crystals evaluated using electron density properties: DFT computations with periodic boundary conditions. J Comp Chem 33 (29):2303-2309. doi:10.1002/jcc.23062

6. Mata I, Alkorta I, Espinosa E, Molins E (2011) Relationships between interaction energy, intermolecular distance and electron density properties in hydrogen bonded complexes under external electric fields. Chem Phys Lett 507:185-189

7. Espinosa E, Molins E, Lecomte C (1998) Hydrogen bond strengths revealed by topological analyses of experimentally observed electron densities. Chem Phys Lett 285:170-173

8. Iogansen AV (1999) Direct proportionality of the hydrogen bonding energy and the intensification of the stretching v(XH) vibration in infrared spectra. Spectrochim Acta A 55 (7-8):1585-1612. doi:10.1016/s1386-1425(98)00348-5

9. Rozenberg M, Loewenschuss A, Marcus Y (2000) An empirical correlation between stretching vibration redshift and hydrogen bond length. Phys Chem Chem Phys 2 (12):2699-2702. doi:10.1039/B002216k

10. Bolis V, Fubini B, Marchese L, Martra G, Costa D (1991) Hydrophilic and hydrophobic sites on variously dehydrated crystalline and amorphous silicas. J Chem Soc Faraday Trans 87:497-505

11. Ugliengo P, Viterbo D, Chiari G (1993) MOLDRAW: Molecular Graphics on a Personal Computer. Z Kristallogr 207:9-23

12. Dovesi R, Orlando R, Erba A, Zicovich-Wilson CM, Civalleri B, Casassa S, Maschio L, Ferrabone M, De La Pierre M, D'Arco P, Noël Y, Causà M, Rérat M, Kirtman B (2014)

CRYSTAL14: A program for the ab initio investigation of crystalline solids. Intern J Quantum Chem 114 (19):1287-1317. doi:10.1002/qua.24658
13. Dovesi R, Saunders VR, Roetti C, Orlando R, Zicovich-Wilson CM, Pascale F, Civalleri B, Doll K, Harrison NM, Bush IJ, D'Arco P, Llunell M, Causà M, Noël Y (2014) CRYSTAL14 User's Manual. University of Torino, Torino
14. Pisani C, Dovesi R, Roetti C (1988) Hartree-Fock ab initio treatment of crystalline systems. In: Lecture notes in Chemistry, vol 48. Springer-Verlag, Berlin, p 193
15. Civalleri B, D'arco P, Orlando R, Saunders VR, Dovesi R (2001) Hartree-Fock geometry optimization of periodic systems with the CRYSTAL code. Chem Phys Lett 228:131-138
16. Schäfer A, Horn H, Ahlrichs R (1992) Fully Optimized Contracted Gaussian-Basis Set for Atoms Li to Kr. J Chem Phys 97:2571-2577
17. Civalleri B, Zicovich-Wilson CM, Valenzano L, Ugliengo P (2008) B3LYP augmented with an empirical dispersion term (B3LYP-D*) as applied to molecular crystals. Cryst Eng Commun 10:405-410
18. Becke AD (1993) Density-functional thermochemistry. III. The role of exact exchange. J Chem Phys 98:5648-5652
19. Lee CT, Yang WT, Parr RG (1988) Development of the Colle-Salvetti Correlation-Energy Formula into a Functional of the Electron-Density. Phys Rev B 37 (2):785-789
20. Monkhorst HJ, Pack JD (1976) Special Points for Brillouin-Zone Integrations. Phys Rev B 13 (12):5188-5192
21. Dovesi R, Saunders VR, Roetti C, Orlando R, Zicovich-Wilson CM, Pascale F, Civalleri B, Doll K, Harrison NM, Bush IJ, D'Arco P, Llunell M (2009) CRYSTAL09 User's Manual. University of Torino, Torino
22. Tosoni S, Pascale F, Ugliengo P, Orlando R, Saunders VR, Dovesi R (2005) Quantum mechanical calculation of the OH vibrational frequency in crystalline solids. Mol Phys 103 (18):2549-2558
23. Dall'Olio S, Dovesi R, Resta R (1997) Spontaneous Polarization as a Berry Phase of the Hartree-Fock Wave Function: The Case of KNbO3. Phys Rev B 56:10105–10114
24. Gatti C, Saunders VR, Roetti C (1994) Crystal field effects on the topological properties of the electron density in molecular crystals: The case of urea. J Chem Phys 101 (12):10686-10696. doi:doi:http://dx.doi.org/10.1063/1.467882
25. Gatti C, Casassa S (2013) TOPOND-2013 : an electron density topological program for systems periodic in N (N=0-3) dimensions, User's Manual - CNR-CSRSRC, Milano, Italy

26. Bader RFW (1990) Atoms in Molecules. A quantum Theory. Oxford University Press, Oxford, UK

27. Gatti C (2005) Chemical bonding in crystals: new directions. Z Kristallogr 220 (5-6):399-457. doi:10.1524/zkri.220.5.399.65073

28. Banerjee A, Adams N, Simons J, Shepard R (1985) Search for stationary points on surfaces. J Phys Chem 89 (1):52-57. doi:10.1021/j100247a015

29. Popelier PLA (1994) A robust algorithm to locate automatically all types of critical points in the charge density and its Laplacian. Chem Phys Lett 228 (1–3):160-164. doi:http://dx.doi.org/10.1016/0009-2614(94)00897-3

30. Tsendra O, Scott AM, Gorb L, Boese AD, Hill FC, Ilchenko MM, Leszczynska D, Leszczynski J (2014) Adsorption of Nitrogen-Containing Compounds on the (100) alpha-Quartz Surface: Ab Initio Cluster Approach. J Phys Chem C 118 (6):3023-3034. doi:10.1021/jp406827h

31. Ugliengo P, Pascale F, Merawa M, Labeguerie P, Tosoni S, Dovesi R (2004) Infrared spectra of hydrogen-bonded ionic crystals: Ab initio study of $Mg(OH)_2$ and β-$Be(OH)_2$. J Phys Chem B 108 (36):13632-13637. doi:Doi 10.1021/Jp047514v

32. Pascale F, Tosoni S, Zicovich-Wilson CM, Ugliengo P, Orlando R, Dovesi R (2004) Vibrational spectrum of brucite, $Mg(OH)_2$: a periodic ab initio quantum mechanical calculation including OH anharmonicity. Chem Phys Lett 396 (4-6):308-315